# Simulation of a Magnetocaloric Heat Pump in Building Technology

S. SCHUH, T. SCHOBERER, L. ZECHNER
*Forschung Burgenland GmbH, Pinkafeld, Österreich*
W. STUTTERECKER
*Fachhochschule Burgenland GmbH, Pinkafeld, Österreich*

ABSTRACT: Increased quality of building envelopes in the last decades leads to decreased heating demands of new buildings and therefore heating devices with lower heating powers are needed. There is a lack of suitable solutions in the heating market in the small power range, which can cover small heating loads decentral without distribution losses. In the presented study, the potential of magnetocaloric heating is investigated. Apart from the advantage that no climate-relevant gases are used compared to commonly used compression heat pumps, this technology is suitable for covering low heating requirements. A cornerstone of the investigation is the development of a programme for simulating the behaviour of a building-integrated magnetocaloric heat pump. Target is to determine the effect of the change in basic properties such as the nature of the magnetocaloric material, the magnetic flux density, the working frequency, etc., but also to determine the influence of building parameters on the overall efficiency of the heating system.

## 1. INTRODUCTION

The magnetocaloric effect describes the behaviour of a solid body that exhibits an increase in temperature when a magnetic field is applied. In 1843, J. Joule observed this effect for the first time. Almost 80 years later, P. Debye and W. Giauque discussed the application of this effect in low-temperature physics to reach temperatures close to the absolute zero point. The experimental proof followed in the year 1933. Four decades later, G. Brown constructed and tested the first refrigerator based on the magentocaloric effect, which was working near room temperature. By the discovery of the giant magnetocaloric effect in 1997, there was a strong increase in research in the field of magnetocaloric cooling, but also concepts for magnetocaloric heat pumps were investigated more intensively (Kitanovski et al., 2015).

In addition to the silent and vibrationless operation of magnetocaloric heat pumps, a great advantage is that no substances with ozone depletion or global warming potential are required. By varying the amount of magnetocaloric material, the heating power can be adapted to the respective requirements. Therefore, this technology is well suited to serve the market for heating devices with low heating power. In order to evaluate the efficiency of magnetocaloric heat pumps, a simulation programme for the performance mapping and parameter optimisation was developed within the scope of the presented study.

## 2. BASICS OF MAGNETOCALORICS

In order to understand the temperature change of a magnetocaloric material (MCM) with a varying magnetic field, one has to consider the entropy of the system. In a simplified picture, the total entropy in a solid body can be divided into the entropy of the nuclei, the electrons, and the electron spin with the associated magnetic moments (Fultz, 2014). When a magnetic field is applied to a MCM, the magnetic moments are aligned, resulting in a decrease in the magnetic entropy. According to the second main theorem of thermodynamics, the total entropy of the system must not decrease. The decrease in magnetic entropy is compensated by an increase of the nuclei entropy via phonon excitation. Phonons describe the elementary excitation of an elastic field, as it is the case for a crystal lattice of a solid body. Therefore, an increase in nuclei entropy leads to an increase in the atomic movement in the solid body, which in turn corresponds to a temperature increase. When switching of the magnetic field, the magnetic moments disorder again, leading to an increase of the magnetic entropy. This entropy change is compensated by a reduction of the nuclei entropy, resulting in a cooling of the material. In Figure 1 the heating process of a MCM by applying a magnetic field is shown schematically.

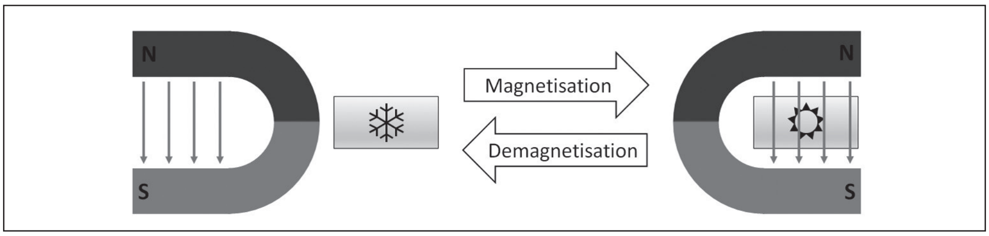


*Figure 1: Heating/cooling of a magnetocaloric material by magnetisation/demagnetisation.*

## 3. WORKING PRINCIPLE OF A MAGNETOCALORIC HEAT PUMP

The alternating heating and cooling of the MCM by the variation of the applied magnetic field can be used for the construction of a heat pump to transfer heat from a low to a high temperature level in a circular process. In general, this process can be divided into the following four steps:

- Activation of the magnetic field and adiabatic heating up of the MCM
- Heat transfer from MCM to a heating system at high temperature
- Deactivation of the magnetic files and adiabatic cooling down of the MCM
- Heat transfer from a heat reservoir at low temperature to the MCM

In literature, this kind of duty cycle can be found under the name Brayton-like cycle (Kitanovski et al., 2015). Figure 2 depicts the T-s-diagram of this operation cycle. Since, the magnetisation (a-b) and demagnetisation (c-d) is considered as an adiabatic process, the entropy stays constant, which leads to a curve progression parallel to the temperature axis.

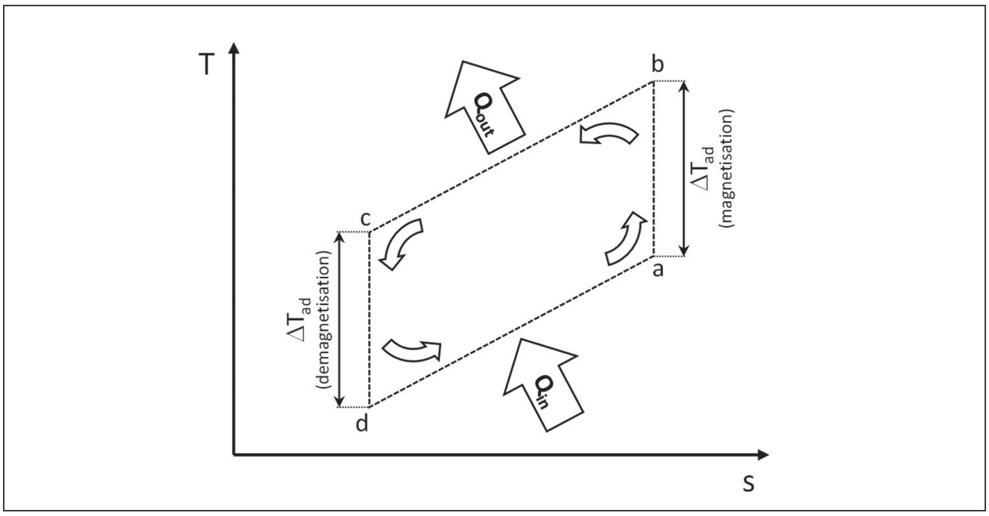


*Figure 2: Schematic example of a Baryton-like cycle in the T-s diagram.*

The extent, to which the temperature changes when a magnetic field is applied, depends on the type of MCM, the magnetic flux density, but also on the temperature of the MCM. A critical parameter in this regard is the Curie temperature. It defines the temperature at which the ferromagnetic property of a material vanishes and it becomes paramagnetic. In Table 1 the Curie temperature of several ferromagnetic materials are listed.

*Table 1: Curie temperature of several ferromagnetic materials (Eichler et al., 2015)*

| Element | TC [K] | Element | TC [K] |
|---|---|---|---|
| Cobalt | 1.423 | Gadolinium | 293 |
| Iron | 1.043 | Dysprosium | 85 |
| Nickel | 627 | Holmium | 20 |

Gadolinium is the only pure material, that shows a transition from ferromagnetism to paramagnetism in the range of room temperature and is therefore of great interest for the investigation of the magneto-caloric effect. Around the Curie temperature, the specific heat of Gadolinium shows a significant change. The curve shape of the specific heat as function of the temperature can significantly be modified by the application of a magnetic field as it is shown on the left side of Figure 3. Based on the specific heat change by the application of a magnetic field, the change in temperature of the MCM is calculated with the formula

$$ {}_{B_0}^{B_1}\delta T_{ad}(T) = \frac{T}{c(T,B_0)} \cdot \int_0^T \frac{c(T,B_0) - c(T,B_1)}{T}\, dT \tag{1} $$

with the change of the magnetic flux density from $B_0$ to $B_1$, the adiabadic temperature change $\delta T_{ad}$ and the temperature T and the specific heat c of the MCM (Risser et al., 2010). The resulting temperature change is plotted on the right side of Figure 3.

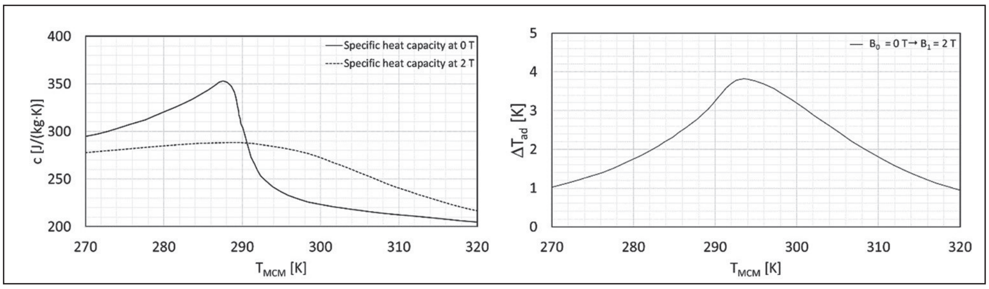


*Figure 3: Specific heat of Gadolinium as function of the MCM temperature and magnetic flux density (left); adiabatic temperature change of Gadolinium (right) induced by the magnetic flux density increase from 0 to 2 T (Risser et al., 2010).*

## 4. SIMULATION

When designing a magnetocaloric heat pump, a huge number of parameters influencing the efficiency of the heat pump, has to be defined. As an example, the quantity and type of magnetocaloric material has to be determined, but also the working frequency, the desired temperature difference or the optimum mass flow rate of the heat transfer fluid are critical for the achieved heat pump performance. In order to limit the value range of the parameters and finally to make a statement about the achievable performance of the magnetocaloric heat pump, the simulation programme presented here was developed.

### 4.1 OPERATION CYCLE

Based on the Brayton-like operation cycle, the sequence of the simulation programme can be divided into four parts, which are shown schematically in the Figure 4. In order to achieve a high heat transfer from the MCM to the heat transport fluid, the MCM is designed as a porous material, which is flown through by the fluid. This structure of the MCM is also called an active magnetic regenerator (AMR). In the first step, the AMR is heated adiabatically by applying a magnetic field. In the second step, fluid from buffer tank 1 with the temperature of the ground collector is flowing through the AMR, leading to a temperature increase of the fluid and cooling down of the AMR. By using a heat exchanger, the fluid emits heat to the heating system and is then stored in the buffer tank 2. After the fluid flow has been stopped, the magnetic field is decreased or deactivated in the third step, which leads to cooling down of the AMR. In the fourth step, fluid flows from the buffer tank 2 in the opposite direction through the AMR and is thereby cooled. After the fluid temperature has been raised by means of a ground collector, it is stored in buffer tank 1 again.

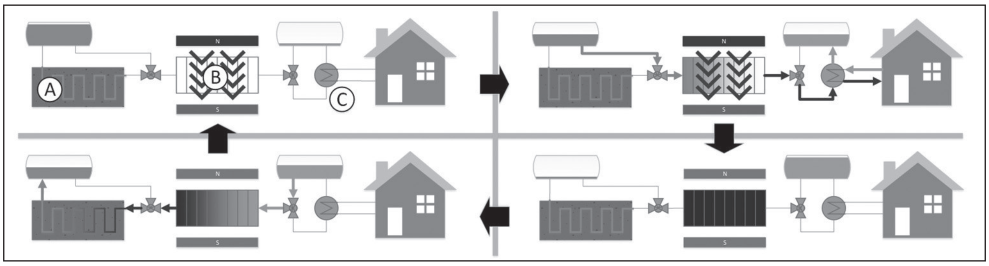


*Figure 4: Schematic representation of the magnetocaloric heat pump operation steps with the ground collector (A), the active magnetic regenerator (B) and the heat exchanger (C).*

### 4.2 PROGRAMME SEQUENCE

For the development of the simulation programme, the software environment MATLAB® was used. The structure of the programme code is illustrated by means of a flow diagram in Figure 6. Initially, all parameters are defined which remain unchanged over the entire simulation time. The next step is the definition of the variable parameters. With the current version of the programme, it is possible to define two variable parameters. The first partial cycle starts with the setting of the starting condition and the activation of the magnetic field. After calculating the temperature change of the AMR due to the magnetic flux change, the determination of the specific heat capacity is performed at the newly set temperature. This is followed by the flow of the fluid through the AMR. For the calculation of the heat transfer from the AMR to the fluid, a discretization of the fluid flow takes place. For this purpose, the AMR is divided into segments with the width dx. With the aid of the fluid mass flow rate and the average channel size through the AMR, which depends on the AMR porosity, it can now be calculated how many AMR segments are traversed by the fluid per time step dt. The shifting process is assumed to be instantaneous. After the fluid has been shifted, the heat transfer between AMR and fluid and the AMR segments is calculated in the time interval dt. This is followed by the calculation of the AMR and fluid temperature change and the change of the AMR specific heat. Next, the fluid is pushed further and the heat transfer is calculated again. Figure 5 shows schematically the heat flow between the AMR segments and between the AMR segments and the fluid.

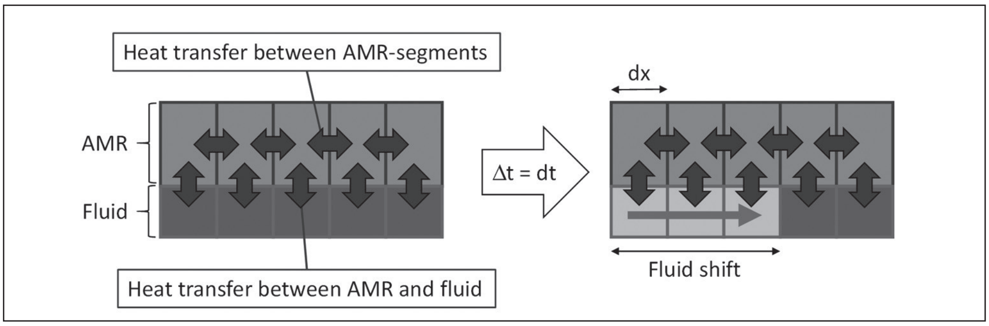


*Figure 5: Schematic representation of the heat transfer between the AMR segments and the fluid and the AMR segments among themselves. Exemplary the right side of the picture shows the instantaneous fluid shift by 3·dx after the time period dt.*

How often the shifting process is repeated depends, on the one hand, on the cycle frequency, on the other hand on the choice of the time interval dt. The smaller the segment size dx and the time interval dt, the smaller are the deviations compared to a continuously running process, but the higher is the required computation time. If the parameters dx and dt are selected too large, instabilities may occur and the simulation result loses its significance. It is therefore important to find a good compromise in the parameter selection with regard to the computation time and the fulfilment of the stability criterion.

The fluid discharged from the AMR is further directed to a counterflow heat exchanger. Depending on the number of transfer units of the heat exchanger, the specific heat capacity, the mass flow rate and the temperature of the fluids on both sides, the heat transfer and the resulting temperature change of the fluids are calculated (Marek & Nitsche, 2015). When all fluid shifts have been carried out, a new partial cycle is started in which the liquid flows in the opposite direction through the AMR. After the magnetic field and therefore the temperature and specific heat of the AMR has been changed, the heat transfer between the fluid and the AMR and its impact on the temperature and the specific heat is calculated in discrete steps in the same way as explained before. The AMR inlet temperature of the fluid corresponds to the average temperature of the fluid that was leaving the heat exchanger in the previous partial cycle. After passing through the AMR, the fluid is directed into a ground collector. The amount of fluid leaving the AMR and the mean temperature differences between the fluid and the soil is determined, followed by the calculation of the heat quantity extracted from the soil.

In the current programme version, an infinitely large earth collector is assumed so that the fluid leaves the collector always at ground temperature level, regardless of the fluid inlet temperature and mass flow rate. After the complete fluid volume has passed through the AMR, the current partial cycle ends and a Brayton-like cycle is completed. Based on the calculated heat flows, the achieved coefficient of performance (COP) and the degree of quality of the magnetocaloric heat pump are determined at the end of each Brayton-like cycle. Depending on the desired temperature difference, the mass flow rates, the working frequency, and many other parameters, it may take up to several hundred Brayton cycles before the system is in steady state and the simulation provides stable values. In order to ensure that the values are stable, a stability check function is integrated which, depending on the specified tolerance, issues a warning when the stability criterion is not reached. After all cycles have been passed, the required simulation results are stored, the simulation parameters are changed according to the predetermined variable parameters and a new simulation run is started.

### 4.3 EXEMPLARY SIMULATION AND ANALYSIS

By way of illustration, the results of an exemplarily simulation are shown in the following. The mass flow rate of the fluid through the AMR, as well as the working frequency of the magnetocaloric heat pump, were defined as variable parameters. A complete overview of the simulation parameters can be found in Table 2.

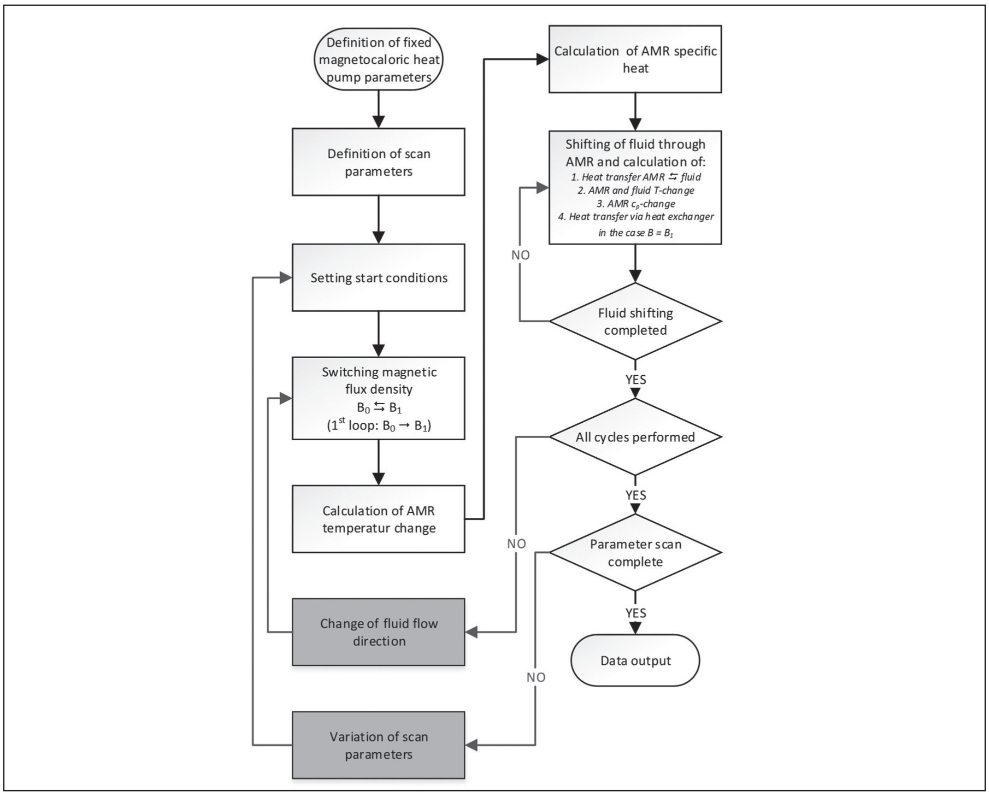


*Figure 6: Flow chart of the magnetocaloric heat pump simulation programme.*

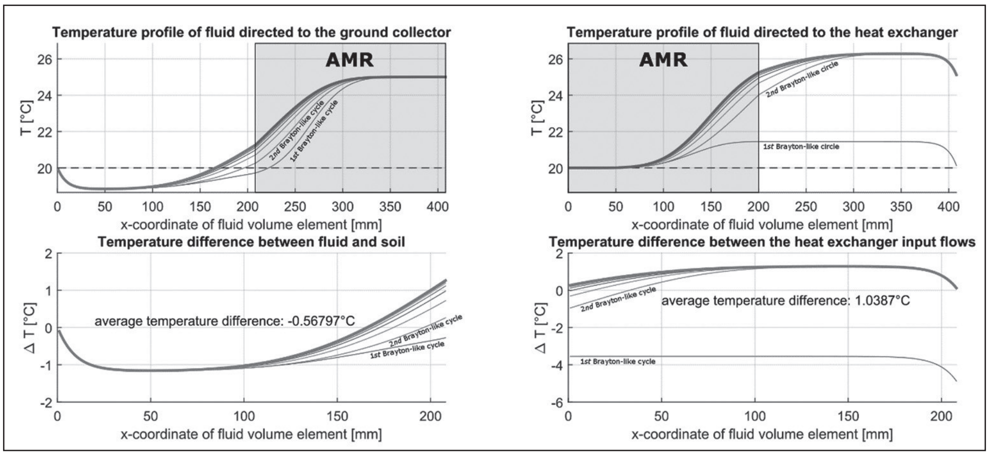


*Figure 7: Temperature profiles in and outside of the AMR of the fluid directed to the ground collector (top left) and the heat exchanger (top right); temperature difference between fluid and soil (bottom left) and between the inlet fluid flows of the heat exchanger (bottom right).*

*Table 2: Simulation parameter overview*

| Parameter | Value/property |
|---|---|
| AMR mass | 5 kg |
| AMR material | Gadolinium |
| AMR segment length dx | 0,53 mm |
| Cycles per parameter set | 250 |
| Density of Gadolinium | 7.886 kg/m³ |
| Density of fluid | 1.089 kg/m³ |
| Fluid temperature from heating system to heat exchanger | 25 °C |
| Heat exchanger transfer surface[1] | 40 m² |
| Heat transfer coefficient between AMR and fluid | 3.000 W/(m²*K) |
| Heat transfer coefficient of heat exchanger | 3.800 W(m²*K) |
| Heat Transfer fluid | Zitrec S-10 |
| Magnetic flux density B0 | 0 T |
| Magnetic flux density B1 | 2 T |
| Mass flow rate of fluid through AMR | 0,05 – 0,7 kg/s |
| Mass flow rate of heating system fluid | 1 kg/s |
| Side length of cubic AMR | 106,6 mm |
| Soil temperature | 20 °C |
| Specific heat of fluid | 3.630 J/(kg*K) |
| Time resolution dt | 1 ms |
| Working frequency | 0,04 – 2 Hz |

[1] chosen very large to avoid heat exchanger influences on total performance for this simulation

Figure 7 shows the spatial temperature distribution of the heat transfer fluid in and outside of the AMR exactly at the time, when the fluid flow is stopped. In the shown case, the simulated mass flow rate of the fluid through the AMR is 0,39 kg/s at a working frequency of 0,3 Hz. It is easy to see that a steeper temperature gradient builds up in the AMR with each subsequent cycle until a constant temperature profile is obtained after about 10 cycles. The average temperature difference between the soil and the fluid emerging from the AMR is 0.57 °C. A temperature difference of about 1 °C can be determined between the inlet flows of the heat exchanger.

On the basis of the temperature profiles it can be identified that the mass flow rate was slightly too large or the working frequency a bit too small selected for the case considered. This is reflected in the fact that the last fluid volume elements flowing out of the AMR toward the ground collector are already at a higher temperature than the soil, thereby releasing heat to the soil instead of absorbing heat.

The calculated COP as a function of the mass flow rate of the fluid through the AMR and the working frequency of the magnetocaloric heat pump is shown in a three-dimensional plot in Figure 8. If only this plot is considered, the wrong conclusion would be drawn and a low flow rate and operating frequency would be considered as the optimum working range for the heat pump. However, when considering the temperature differences between the inlet fluid flows of the heat exchanger in Figure 9, it can be seen that the achieved temperature difference is in the range of 0,1 to 0,2 K for low mass flow rates and working frequencies. It is therefore necessary to find a compromise between the desired temperature elevation and the achieved COP.

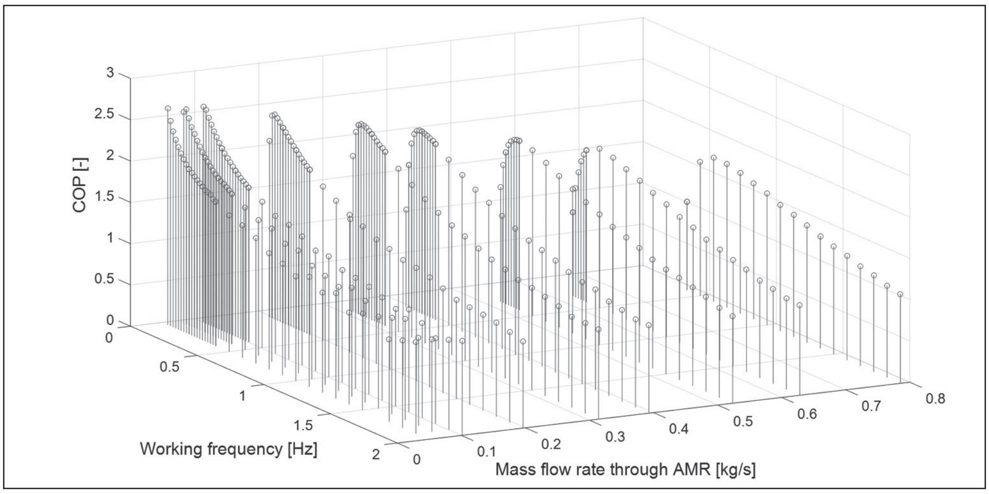


*Figure 8: COP as function of the fluid mass flow rate through the AMR and the working frequency of the magnetocaloric heat pump.*

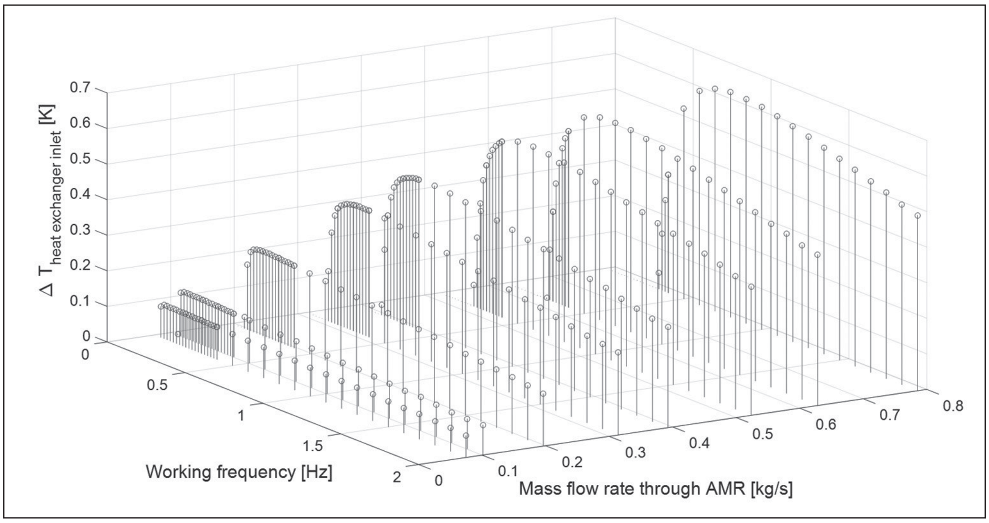


*Figure 9: Temperature difference between the inlet flows of the heat exchanger as function of the mass flow rate through the AMR and the working frequency of the magnetocaloric heat pump.*

Considering the temperatures of the AMR occurring during the simulation, values between 19 °C and 29 °C are reached. Assessing the adiabatic temperature change of gadolinium when changing the magnetic flux from 0 to 2 T (see right side of Figure 3), one can observe that at a starting temperature of 29 ° C, the adiabatic temperature change is reduced to 2,8 °C compared to the maximal achievable value of 3,8 °C. This deteriorates even further, the higher the desired starting temperature is. This has the following consequences: On the one hand, a strong temperature gradient within the AMR leads to the fact that only a narrow spatial range of the AMR is operating in the optimum temperature window. On the other hand, the efficiency of the magnetocaloric heat pump at operating temperatures higher than 30 °C, as needed for heating purposes, will drop significantly. A solution of this problem is provided by splitting the AMR is several MCM layers whose Curie temperatures are matched to the respective temperature range. For this purpose, it is necessary not to use a pure substance like Gadolinium, but rather alloys whose curie temperature can be adjusted per composition. Examples of such alloys and their Curie temperatures are given in Table 3.

*Table 3: MCM-alloys with a Curie temperature $T_C$ higher than 15 °C (Kitanovski et al., 2015)*

| MCM | $T_C$ [K] | MCM | $T_C$ [K] |
|---|---|---|---|
| $LaFe_{10.96}Co_{0.97}Si_{1.07}$ | 289 | MnAs | 318 |
| $La(Fe_{0.89}Si_{0.11})_{13}H_{1.3}$ | 291 | $MnFeP_{0.45}As_{0.55}$ | 306 |
| $La(Fe_{0.88}Si_{0.12})_{13}H_{1.5}$ | 323 | $Mn_{1.1}Fe_{0.9}P_{0.47}As_{0.53}$ | 292 |

## 5. CONCLUSION AND OUTLOOK

In the presented study, the development of a programme for the simulation of a magnetocaloric heat pump was presented. The aim is to use the programme to assess the achievable efficiency and temperature differences. For this purpose, fixed and variable operating parameters are defined in order to carry out a performance scan. With the help of the simulation results, it is now possible to narrow down the range of values of the parameters and to find the optimum parameter configuration in a time-efficient manner. It was found that with an AMR, which consists of only one MCM, the maximum temperature difference is strongly limited by the fact that the magnetocaloric effect decreases noticeably with a greater deviation of the MCM temperature from the Curie temperature. The problem can be solved by using a series of MCMs with adapted Curie temperatures instead of only one MCM. After the desired temperature profile within the AMR is determined with the actual simulation programme, the AMR model will be adapted to this profile in a further software development step to increase the heat pump efficiency and the achievable temperature difference.

## ACKNOWLEDGMENT

This investigation was carried out within the project Future_Heat_Pump, which is funded by the programme COIN by BMWFW.

## LITERATURE

Eichler, H., Oppen, G., & Luders, K. (2015). Relativistische Physik - von der Elektrizität zur Optik Walter De Gruyter.

Fultz, B. (2014). Phase transitions in materials (1. publ. ed.). Cambridge: Cambridge Univ. Press.

Kitanovski, A., Tušek, J., Tomc, U., Plaznik, U., Ožbolt, M., & Poredoš, A. (2015). Magnetocaloric Energy Conversion. Cham: Springer.

Marek, R., & Nitsche, K. (2015). Praxis der Wärmeübertragung (4., neu bearbeitete Auflage ed.). München: Fachbuchverlag Leipzig.

Risser, M., Vasile, C., Engel, T., Keith, B., & Muller, C. (2010). Numerical simulation of magnetocaloric system behaviour for an industrial application. International Journal of Refrigeration, 33(5), 973-981. doi:10.1016/j.ijrefrig.2010.02.004

*Contact Author*
*Sebastian Schuh*
*Steinamangerstraße 21*
*7423 Pinkafeld*
*Austria*
*E-Mail: sebastian.schuh@forschung-burgenland.at*